Design Reference Mission Case Study
Stratospheric Observatory for Infrared Astronomy Science Steering Committee

Spatially Resolved Protostars in Taurus

Program contacts: Lynne Hillenbrand, Joshua Eisner
Scientific category: STAR FORMATION
Instruments: FORCAST, HAWC
Hours of observation: 39

Abstract

We propose mid- and far-infrared imaging observations of Class I protostars in the Taurus-Auriga star-forming region. Combined with spatially resolved scattered light images at optical and near-infrared wavelengths, marginally spatially resolved thermal images at millimeter wavelengths, and broadband spectral energy distributions (SEDs) over 4-5 decades in wavelength, SOFIA images near the wavelength of peak emission in the SED will be used to constrain circumstellar geometry in ways not possible from previous imaging datasets or SEDs alone. In particular, these observations will provide unique information on the size distribution of circumstellar grains by potentially spatially resolving the mid-infrared continuum emission. Further, by finely sampling the spectral energy distribution over the peak emission wavelengths, SOFIA/FORCAST and SOFIA/HAWC data will yield the most accurate source luminosities derived to date for Class I protostars.

Observing Summary:

Target	RA	Dec	F_{Jy}	Configuration/m
IRAS 04016+2610	04 04 42.9	+26 18 56	10.63 at 21μm, 62.28 at 100μm	6 FORCAST, 4
IRAS 04108+2803	04 13 54.69	+28 11 33.1	2.61 at 21μm, 10.82 at 100μm	6 FORCAST 4 I
IRAS 04239+2436	04 26 56.28	+24 43 35.6	4.43 at 21μm, 17.15 at 100μm	6 FORCAST 4 I
IRAS 04295+2251	04 32 32.04	+22 57 26.7	10.63 at 21μm, 8.21 at 100μm	6 FORCAST 4 I
IRAS 04381+2540	04 41 12.68	+25 46 35.5	0.20 at 21μm, 14.93 at 100μm	6 FORCAST 4 I
				Grand total hour

Scientific Objectives

The canonical picture of low-mass star formation is that of a rotating, collapsing cloud of dust and gas that forms a protostar surrounded by a disk (e.g., Terebey et al. 1984; Shu et al. 1987, 1993). Different stages of this theoretical evolutionary process have been equated with observed differences in the SEDs of protostellar objects, which have been grouped into classes 0-III based on their infrared spectral index and the ratio of sub-millimeter to bolometric luminosity (Lada & Wilking 1984; Lada 1987; Adams et al. 1987; André et al. 1993). In this classification scheme, Class 0 and I sources are still in the main accretion phase, and emit most of their radiation at far-IR and submm wavelengths due to reprocessing of light from the central protostars by dust grains in the infalling envelope. In contrast, Class II and III sources exhibit directly revealed pre-main-sequence stars in addition to emission from circumstellar disks.

This classification scheme is an attempt to represent discretely a continuous evolutionary sequence, and there are transition objects that create some blur between classes. Moreover, this sequence is defined solely from spatially unresolved spectral energy distributions (SEDs), which contain only limited information about the circumstellar distributions. Thus, it is not clear that the observed differences in SEDs truly correspond to evolutionary changes in the circumstellar geometry. A crucial test is to constrain the geometry of material around members of these different evolutionary classes using spatially resolved images, and thereby either confirm or refute the evolutionary sequence inferred from spatially-unresolved SEDs.

Direct and interferometric imaging of Class II sources has shown that the bulk of the circumstellar material lies in disks (e.g., McCaughrean & O'Dell 1996; Koerner & Sargent 1995; Eisner et al. 2003, 2004), while there may be a small amount of material in tenuous envelopes (e.g., Grady et al. 1999; Semenov et al. 2004). Thus, Class II sources appear to be fully-assembled young stars surrounded by rotating disks from which they continue to accrete material. Direct images of the less evolved Class I sources are relatively rare compared to the Class II sources, due to the large extinctions to these embedded objects, and thus the circumstellar geometry for these objects is not well constrained. We focus our proposed study on the geometry of material around these presumably less evolved sources.

Studies of the emergent spectral energy distributions at wavelengths $\gtrsim$ 10 μm have provided important, albeit ambiguous, constraints on the circumstellar dust distributions for Class I objects. Models incorporating infalling, rotating, envelopes with mass accretion rates on the order of 10^{-6} $M_\odot$ yr^{-1} are consistent with observed SEDs (e.g., Adams et al. 1987; Kenyon et al. 1993a), and the compatibility of the derived mass accretion rates with statistically-inferred ages of Class I sources (Adams et al. 1987; Myers et al. 1987; Benson & Myers 1989; Kenyon et al. 1990) provides further support for these envelope models. However, for some objects whose SEDs can be explained by spherically-symmetric dust distributions, it has been suggested that nearly edge-on flared disk models may also be able to reproduce the observed SEDs (Chiang & Goldreich 1999). Observations that spatially resolve the circumstellar emission are necessary to remove the ambiguities inherent in SED-only modeling.

Figure 1: SED data, 10 μm spectrum, 0.9 μm scattered light image, and 1.3 mm continuum image for IRAS 04016+2610, along with best-fit models for different assumed circumstellar geometries. The observed images have been rotated on the sky by $-10°$ (east of north) so that they have the same position angle definition as the models. Images have contour levels of 10% of the peak flux, beginning at 10% for the 0.9 μm images and 30% for the 1 mm images. While pure disk models do not provide an adequate match to the data, extincted disks, pure envelopes, and disk+envelopes match reasonably well. The disk+envelope, which provides the smallest residuals between model and data, is preferred.

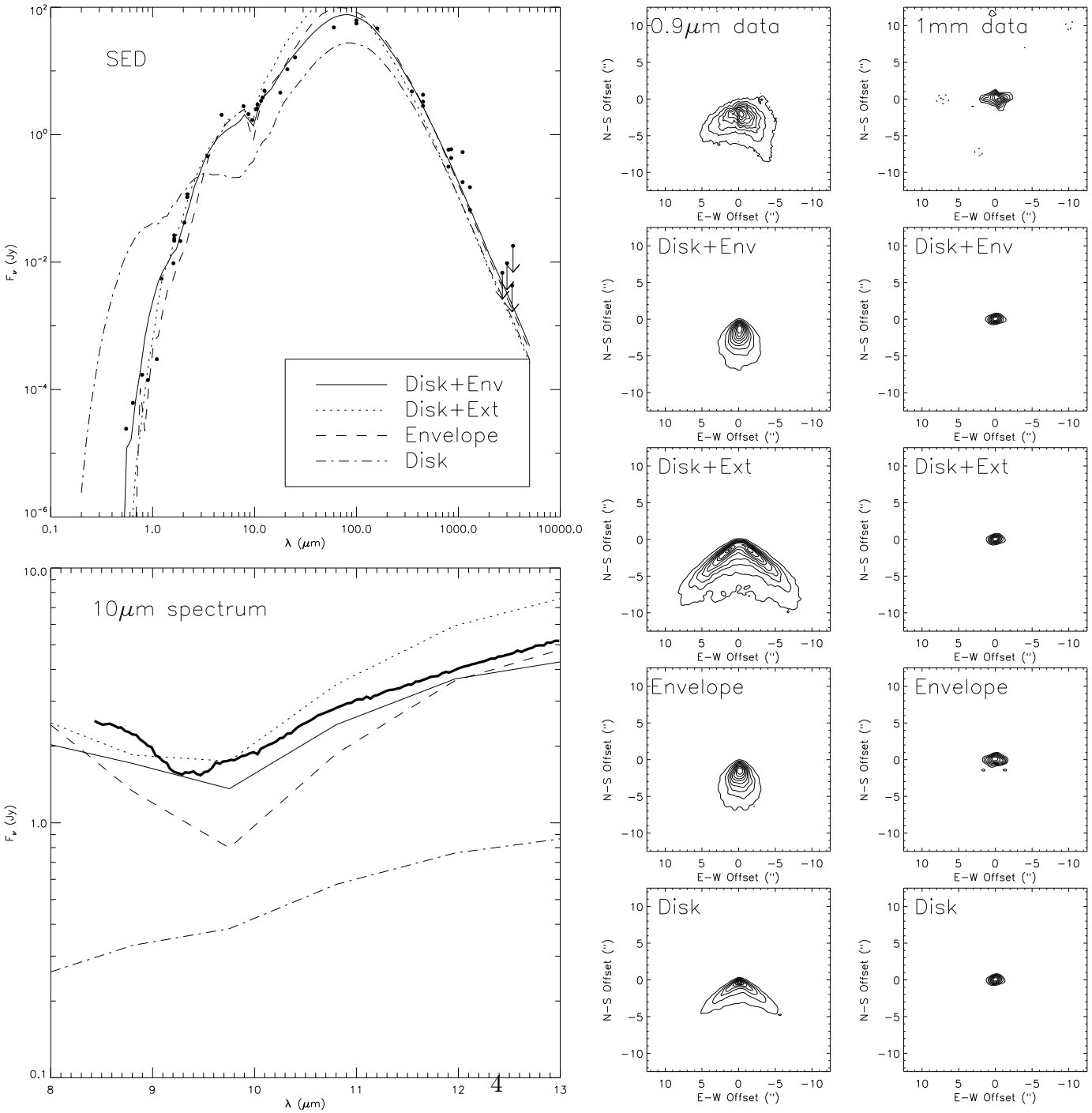

Figure 2: Synthetic images at 70 and 160 μm (top and bottom panels, respectively) for a disk+envelope model of the circumstellar dust distribution around a Class I source. Contours are plotted for values of 1, 10, and 50% of the peak fluxes in the images. The model is similar to the best-fit model for IRAS 04016+2610 shown in Figure 1 and assumes the following circumstellar properties: an envelope infall rate of 6×10^{-6} $M_\odot$ yr^{-1}, a centrifugal radius of 100 AU, a disk mass of 0.03 $M_\odot$, an outer radius of 2000 AU, and a viewing angle inclined by 50°. The dust properties ISM-like. Non-ISM-like dust properties or larger outer radii produce larger images.

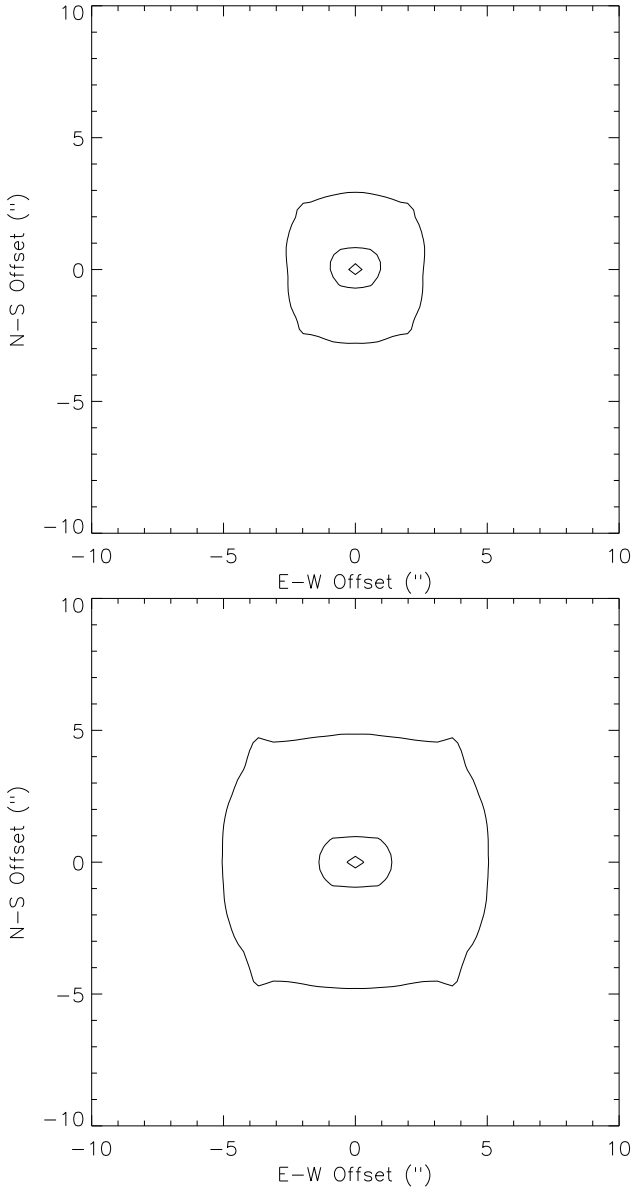

The circumstellar geometry is constrained directly by spatially resolved images of scattered light at near-IR wavelengths (e.g., Kenyon et al. 1993b; Whitney et al. 1997, 2003b), and the asymmetric emission morphologies observed in some sources provide strong evidence that the circumstellar material is not spherically distributed around Class I objects. However, since scattered light traces tenuous dust in the surface layers of circumstellar dust distributions, it does not allow an unambiguous determination of geometry or other circumstellar properties. For example, while spherically-symmetric dust distributions can be ruled out, modeling of scattered light alone can not necessarily distinguish between a flattened envelope and a flared disk.

Modeling of images at multiple wavelengths can provide tighter constraints on geometry, since emission at different wavelengths arises in different layers of the circumstellar material, with short-wavelength scattered light from low-density surface layers and longer-wavelength emission from deeper, cooler layers at larger radii. For the Class I source L1551 IRS 5, spatially resolved observations at several wavelengths (e.g., Strom et al. 1976; Keene & Masson 1990; Butner et al. 1991; Lay et al. 1994; Ladd et al. 1995; Rodriguez et al. 1998; Chandler & Richer 2000; Motte & André 2001) and detailed spectroscopy (White et al. 2000) have been combined with SED modeling, providing important additional constraints on the models (Osorio et al. 2003). Moreover, the combination of low and high resolution millimeter observations facilitated distinction of compact disk emission and more extended envelope emission. Similar modeling of multi-wavelength observations for IRAS 04302+2247 provided firm constraints on the distribution of circumstellar material and the properties of the circumstellar dust grains (Wolf et al. 2003).

In order to further our understanding of the Class I population as a whole, we have obtained high spatial resolution observations at optical and millimeter wavelengths for a sample of protostars classified (e.g. by Kenyon et al. 1993a) as Class I objects. We propose here to obtain complementary mid- and far-infrared images. The short wavlength scattered light images trace the low-density surface layers while thermal mid-infrared images trace the hot inner regions near 1-10 AU, and millimeter images trace cooler layers at larger radii. Because images at these various wavelengths probe different regions of the disk, and even different emission mechanisms, when considered together and in conjunction with SEDS they place tight constraints on the range of circumstellar dust models consistent with the data.

SOFIA can probe wavelengths encompassing the peak of the SEDs for Class I sources. Using the three dimensional radiative transfer code MC3D (Wolf & Henning 2000; Wolf 2003), we will model our data in the context of three types of circumstellar dust distributions: 1) rotating infalling envelopes; 2) flared disks; and 3) combinations of envelopes+disks. Images at FORCAST and HAWC wavelengths for a representative disk+envelope model are quite compact, since the emission traces predominantly the warm inner regions within 100 AU of the central protostar. The FWHM angular sizes for a source at 140 pc are $\sim 0\farcs3$ to $1\farcs2$ or larger at 20-150 μm. Although this is smaller than the angular resolution of *SOFIA* at these wavelengths, the 1% emission contours are comparable to the available angular resolution. The images could appear either unresolved or marginally resolved. However, if the dust properties are substantially different than those of standard ISM grains, *SOFIA*

may be able to significantly resolve some emission. In recent observations of Vega, *Spitzer* 24 μm imaging found the source to be much larger than anticipated based on simple modelling expectations, and suggest that there may be a large population of transiently-heated small dust grains at large radii responsible for the extended mid-IR emission (Su et al. 2005). Class I sources may also be surrounded by large-scale distributions of small dust grains; *SOFIA* observations can test this hypothesis.

References

Adams, F. C., Lada, C. J., & Shu, F. H. 1987, ApJ, 312, 788

André, P., Ward-Thompson, D., & Barsony, M. 1993, ApJ, 406, 122

Benson, P. J. & Myers, P. C. 1989, ApJS, 71, 89

Butner, H. M., Evans, N. J., Lester, D. F., Levreault, R. M., & Strom, S. E. 1991, ApJ, 376, 636

Chandler, C. J. & Richer, J. S. 2000, ApJ, 530, 851

—. 1999, ApJ, 519, 279

Eisner, J. A., Lane, B. F., Akeson, R. L., Hillenbrand, L., & Sargent, A. 2003, ApJ, 588, 360

Eisner, J. A., Lane, B. F., Hillenbrand, L., Akeson, R., & Sargent, A. 2004, ApJ, 613, 1049

Eisner, J. A., Hillenbrand, L.A., Carpenter, J.M. & Wolf, S. 2005, ApJ, submitted

Grady, C. A., Woodgate, B., Bruhweiler, F. C., Boggess, A., Plait, P., Lindler, D. J., Clampin, M., & Kalas, P. 1999, ApJ, 523, L151

Keene, J. & Masson, C. R. 1990, ApJ, 355, 635

Kenyon, S. J., Calvet, N., & Hartmann, L. 1993a, ApJ, 414, 676

Kenyon, S. J., Hartmann, L. W., Strom, K. M., & Strom, S. E. 1990, AJ, 99, 869

Kenyon, S. J., Whitney, B. A., Gomez, M., & Hartmann, L. 1993b, ApJ, 414, 773

Koerner, D. W. & Sargent, A. I. 1995, AJ, 109, 2138

Lada, C. J. 1987, in IAU Symp. 115, Star Forming Regions, ed. M. Peimbert & J. Jugaku (Dordrecht: Reidel), 1

Lada, C. J. & Wilking, B. A. 1984, ApJ, 287, 610

Ladd, E. F., Fuller, G. A., Padman, R., Myers, P. C., & Adams, F. C. 1995, ApJ, 439, 771

Lay, O. P., Carlstrom, J. E., Hills, R. E., & Phillips, T. G. 1994, ApJ, 434, L75

McCaughrean, M. J. & O'Dell, C. R. 1996, AJ, 111, 1977

Motte, F. & André, P. 2001, A&A, 365, 440

Myers, P. C., Fuller, G. A., Mathieu, R. D., Beichman, C. A., Benson, P. J., Schild, R. E., & Emerson, J. P. 1987, ApJ, 319, 340

Osorio, M., D'Alessio, P., Muzerolle, J., Calvet, N., & Hartmann, L. 2003, ApJ, 586, 1148

Rodriguez, L. F., D'Alessio, P., Wilner, D. J., Ho, P. T. P., Torrelles, J. M., Curiel, S., Gomez, Y., Lizano, S., Pedlar, A., Canto, J., & Raga, A. C. 1998, , 395, 355

Semenov, D., Pavlyuchenkov, Y., Schreyer, K., Henning, T., Dullemond, C., & Bacmann, A. 2004, ArXiv Astrophysics e-prints

Shu, F., Najita, J., Galli, D., Ostriker, E., & Lizano, S. 1993, in Protostars and Planets III, 3–45

Shu, F. H., Adams, F. C., & Lizano, S. 1987, ARAA, 25, 23

Strom, K. M., Strom, S. E., & Vrba, F. J. 1976, AJ, 81, 320

Su, K. Y. L., Rieke, G. H., Misselt, K. A., Stansberry, J. A., Moro-Martin, A., Stapelfeldt, K. R., Werner, M. W., Trilling, D. E., Bendo, G. J., Gordon, K. D., Hines, D. C., Wyatt, M. C., Holland, W. S., Marengo, M., Megeath, S. T., & Fazio, G. G. 2005, ArXiv Astrophysics e-prints

Terebey, S., Shu, F. H., & Cassen, P. 1984, ApJ, 286, 529

White, G. J., Liseau, R., Men'shchikov, A. B., Justtanont, K., Nisini, B., Benedettini, M., Caux, E., Ceccarelli, C., Correia, J. C., Giannini, T., Kaufman, M., Lorenzetti, D., Molinari, S., Saraceno, P., Smith, H. A., Spinoglio, L., & Tommasi, E. 2000, A&A, 364, 741

Whitney, B. A., Kenyon, S. J., & Gomez, M. 1997, ApJ, 485, 703

Whitney, B. A., Wood, K., Bjorkman, J. E., & Cohen, M. 2003a, ApJ, 598, 1079

Whitney, B. A., Wood, K., Bjorkman, J. E., & Wolff, M. J. 2003b, ApJ, 591, 1049

Wolf, S. 2003, Computer Physics Communications, 150, 99

Wolf, S. & Henning, T. 2000, Computer Physics Communications, 132, 166

Wolf, S., Padgett, D. L., & Stapelfeldt, K. R. 2003, ApJ, 588, 373

SOFIA Uniqueness/Relationship to Other Facilities

These observations are not feasible from the ground due to the wavelengths involved.

Observing Strategy

Our sample of protostars in Taurus-Auriga spans the range of bolometric luminosities known for the class (0.1-5 $L_{\odot}$) but are the brightest objects of the class at millimeter wavelengths. We propose observations with SOFIA/FORCAST in 6 filters between 5 and 40 μm and SOFIA/HAWC in in 4 filters between 50 and 250μm .

Integration times with SOFIA are quite short for detection only. However, our goal is to constrain the spatial extent of the objects. Generic envelope-plus-disk models of Class I sources (e.g. Eisner et al. 2005) suggest that SOFIA may marginally resolve the Taurus-Auriga Class I sources with non-ISM-like grain size distributions producing larger and hence more resolvable images. Either way, the information is useful for constraining circumstellar dust geometry.

Our integration times are set by requiring detection of the 1% image contour in the generic envelope-plus-disk model at SNR=3-10, dictating SNR=300-1000 on the flux peak. We will observe in the 5.6, 8.6, 11.3, 19.5, 30.7, and 38.0 μm filters with FORCAST and the 53, 88, 155, 215 μm filters with HAWC. Integration times plus overhead total 400-3600 seconds with each FORCAST filter and 900-3600 seconds with each HAWC filter. Our program requires 36 hours of observatory resources for our 5 proposed targets.

Special Requirements

Precursor/Supporting Observations

The proposed SOFIA observations will complement existing spatially resolved data at shorter and longer wavelengths.